Engineering and Technology Journal
Journal homepage: https://etj.uotechnology.edu.iq

Rod-like Nano-structures of Copper Oxide Prepared by Chemical Bath Deposition

Zainab M. Sadiq *, Mustafa A. Hassan, Khaleel I. Hassoon

Applied Sciences Dept., University of Technology-Iraq, Alsina'a street, 10066 Baghdad, Iraq.
*Corresponding author Email: as.19.20@grad.uotechnology.edu.iq

HIGHLIGHTS

- The chemical bath deposited method was used because its simple, easy, and inexpensive.
- A rod-like nano-structure of Copper Oxide was prepared.
- The effect of annealing temperature (400 and 500) was studied.

ARTICLE INFO

Handling editor: Rana F. Ghani

Keywords: Copper oxide; Nano rods; Nanostructure; Chemical bath; deposition method (CBD) ; Crystal Structure.

ABSTRACT

In this paper, we reported that the annealing at temperatures of 400 and 500 oC in the air for 2 hours led to the formation of rod-like structures of cupric oxide thin films prepared by the chemical bath deposition technique. The structure and the optical properties of the prepared thin films were studied to investigate the role of annealing on the films. The morphology of the as-deposited CuO films is almost structureless. However, the films are converted to rod-like shapes nano-structures after annealing, as confirmed by scanning electron microscopy. The x-ray analysis showed that the thin films of copper oxide nano-structures have a monoclinic crystallinity preferred in the (110), (002), and (111) directions, and the crystallinity increases after annealing. Furthermore, the bandgap values after annealing are reduced from 2.1 to 1.61 and 1.63 eV as determined by optical analysis utilizing UV–VIS spectroscopy.

1. Introduction

Nowadays, Nano-science and Nanotechnology are the most common terms because of their versatile applications in many fields of knowledge [1]. The most important fact is that as the bulk materials are decreased to nanoscale dimensions, their properties, which are a function of surface-area-to-volume ratio, change due to quantum confinement effects [2]. Nanostructured transition metal oxides have been studied for their interesting properties and versatile applications. CuO is an important semiconductor with positive conductivity (p-type) and a relatively narrow energy bandgap (1.4–1.7 eV). It has many applications in sensors, batteries, superconductors, optics, photocatalysts, and field emission devices [3]. Copper oxide is also an important candidate for photovoltaic applications [4]. It is well-known that the physical and chemical properties of the CuO are significantly dependent on its microstructures and morphology [5]. As a result, numerous studies have been conducted in recent years to develop novel CuO nano-structures with controlled morphologies and novel physical and chemical properties. Numerous CuO nanostructures including nanowires [6], nanosheets [7], nanotubes [8], nanorods [9] and nanoneedle [10] have been synthesized using various methods such as electro-deposition [11] hydrothermal treatment [12], thermal evaporation [13], thermal oxidation [14], quick-precipitation [15], solution synthesis [16] and high-temperature combustion [17] …etc.

The chemical bath deposition method (CBD) is currently gaining much interest for many reasons. First of all, the starting chemicals used in CBD are widely available and inexpensive. Furthermore, the possibility of preparing pinhole-free and uniform thin films with large areas. Another positive feature is that the deposition temperature is relatively low (90 °C) [18]. Few articles have been published on the growth of rod-like shapes of copper oxide. In particular, Oh, et al. studied the effect of growth time on the CuO nanorods using the CBD method [4]. In the work of Ha et al., Ni-doped CuO nanorods were grown on a CuO film using different nickel amounts via the modified CBD method [19]. The effect of the concentration of copper precursor has also been evaluated [20]. Liu et al. reported the growth of CuO nanorods by a seed-mediated hydrothermal method and studied the effect of the growth temperature (75, 80, and 85 C) [21]. The CBD method was chosen for the synthesis of CuO nanorods, and the role of annealing temperature is investigated in this study.

http://doi.org/10.30684/etj.v40i4.2087
Received 25 March 2021; Accepted 4 July 2021; Available online 25 April 2022
2412-0758/University of Technology-Iraq, Baghdad, Iraq

2. Experimental details

All the chemicals used in the experiments, copper(II) chloride dehydrate ($CuCl_2.2H_2O$), hydrochloric acid (HCl), and ammonia (NH_3), were analytical grade, purchased Sigma–Aldrich. De-ionized (DI) water was used as a solvent throughout the experiment. Figure 1 displays a simple setup for synthesizing CuO thin films on glass slides using the single-step CBD technique. The glass slides are first washed in a dilute hydrochloric acid solution (HCl, 1:5), followed by frequent distilled water rinses, ethanol alcohol rinses, and drying with special cleaning papers. The preparation method is as follows: 1.70 g of copper (II) chloride ($CuCl_2.2H_2O$) is dissolved in 100 ml of de-ionized water to obtain a concentration of 0.1 M. A magnetic stirrer is utilized to mix the solution thoroughly for 1 hour. The resulting solution has a clear blue color at room temperature. Then we change the solution pH to 10 by adding ammonia (NH_3) with 25-30% concentration. The solution starts to boil at around 90°C, and at this point, the substrates should be dipped into it. The time required for boiling is about 7 minutes (i.e., the temperature increases from room temperature to 90°C is about 7 min.). The substrates are removed from the bath after boiling for 2.5 minutes and rinsed in distilled water. Three series of samples were prepared in this work to explore the impact of heat treatments on the films. The first was kept at room temperature (as-deposited film). The second and the third samples were exposed to an annealing process at 400°C and 500°C for 2 hours, respectively.

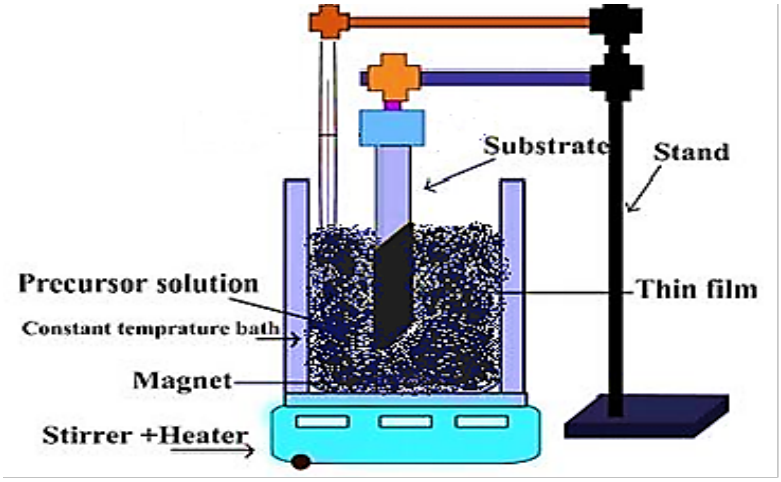

Figure 1: Schematic of a chemical bath method [22]

3. The growth mechanism

The story of the growth mechanism is as follows: $Cu(OH)_2$ precipitates from copper ions in an aqueous solution when the ionic product (IP) of the solution is greater than the solubility product (SP). The degree of supersaturation (S), known as the ratio of IP to SP, is widely accepted as an important parameter for assessing the precipitation process in an aqueous solution. The deposition does not occur if S is less than 1; if S is greater than 1 but less than the critical value of Sc, heterogeneous deposition occurs on the container and substrate walls, as the S value is insufficient to induce nuclei in a bulk solution. On the other hand, if S is greater than S_c, homogeneous sedimentation occurs [23]. According to this theory, the S value for copper ions must be set in the range of 1 to Sc to achieve heterogeneous nucleation on the substrate.$CuCl_2.2H_2O$ was used as an ion source, and NH_3 was used as a reagent in this study. As shown in the equation, Cu^{+2} ions were obtained by dissolving 1.705 g $CuCl_2.2H_2O$ in double-distilled water (1). The pH of the solution was about 3.80 before the precipitation reaction began. The following are some chemical reactions that could occur:

$$CuCl_2.2H_2O \rightarrow Cu^{+2}\,(aq) + 2Cl^{-}(aq) \quad (1)$$

$$NH_3 + H_2O \leftrightarrow NH_4^{+}\,(aq) + OH^{-}\,(aq) \quad (2)$$

$$Cu^{+2}\,(aq) + 2OH^{-}\,(aq) \rightarrow Cu(OH)_2 \quad (3)$$

$$Cu(OH)_2 \rightarrow CuO + H_2O \quad (4)$$

Ammonia plays an important role in creating the desired CuO nano-structures in the proposed reaction scheme. By adding ammonia, which introduces ammonium ions and OH, the pH of the solution is increased to 10.0 (equation (2)). Since this stage regulates the supply of OH ions, which decides the degree of supersaturation S, it is a crucial stage of the chemical reaction. Even in a high OH concentration solution, the $Cu(OH)_2$ precipitate cannot dissolve and form soluble complex ions like $Cu(OH)_4^{-2}$. As a result, we assume that nanoscale CuO crystal cores formed during the dehydration of $Cu(OH)_2$ precipitate and developed on the substrates and container walls over time. This decomposition is caused by subsequent heating of the solution (equation (4)). It was determined that the grown film is entirely made up of CuO molecules based on the X-ray patterns of the synthesized and annealed films.

4. Results and Discussion

4.1 Structural properties

Figure 2 demonstrates X-ray patterns of CuO samples before and after annealing at 400°C and 500°C. The patterns are well fitted to CuO monoclinic crystal phase with peaks at 35.55° and 38.67°, corresponding to (002) and (111) planes. The analyzed diffraction peaks were confirmed with the values available in the JCPDS card No. 45-0937. It can be seen that the annealing temperature influences the XRD pattern of copper oxide films, i.e., the intensity of the noticed peaks (thus crystallinity of the thin films) increases with the annealing temperature. No conspicuous pinnacle shift related to Cu_2O phase or recognizable impurities were identified with an increment in the annealing temperature. It can be deduced from the XRD patterns that annealing improves the crystallinity and the purity of the CuO formation process [24].

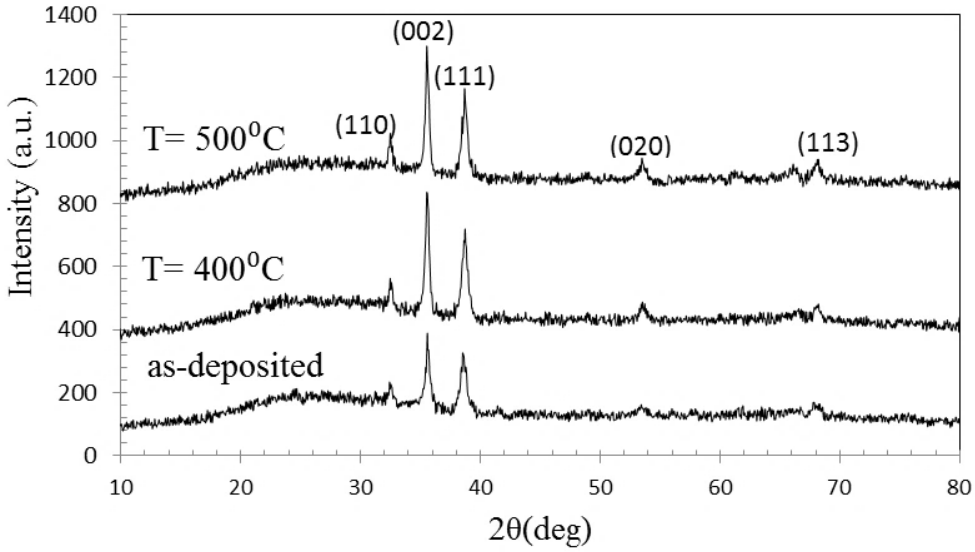

Figure 2: Three x-ray patterns for CuO

Figure 3: prepared by CBD technique, and two of them annealed at two different temperatures

The crystallite size (D_{ave}) is calculated using Scherrer's relation, and the dislocation density (δ) was obtained using Eq. (2) below [25], and the results are shown in Table 1.

$$D_{ave} = \frac{K\lambda}{\beta cos\theta} \quad (5)$$

$$\delta = \frac{1}{D_{ave}^2} \quad (6)$$

where K is a constant and λ =1.5406 Å is the Kα wavelength of the x-ray, θ is the Bragg diffraction angle, β (in radians) is the full width at half maximum.

Table 1 displays the results as a function of annealing temperature. The improvement in size is primarily due to increased crystallinity and reduced defect density in CuO films [15-17].

Table 1: Summarized results of CuO thin films prepared by CBD technique and annealed at two different temperatures

T(°C)	(hkl)	2θ(degree)	Aspect Ratio(nm)	δ (nm)$^{-2}$	RMS(nm)	E_g(eV)
As-deposited	(002)	35.62		5.5×10^{-4}	2.83	2.2
	(111)	38.60		2.2×10^{-3}		
400°C	(110)	32.52	438:92	1.2×10^{-3}	6.59	2.1
	(002)	35.58		1.2×10^{-3}		
	(111)	38.72		2.1×10^{-3}		
	(020)	58.57		3.0×10^{-4}		
500°C	(110)	32.47	360:121	1.2×10^{-3}	8.17	1.8
	(002)	35.54		1.7×10^{-3}		
	(111)	38.69		5.4×10^{-3}		
	(020)	58.55		7.8×10^{-3}		
	(113)	68.2		5.6×10^{-3}		

4.2 Surface morphology

Field emission scanning electron microscopy (FESEM), accompanied by EDX, was used to investigate the structure and morphology of the CuO thin film. FESEM micrographs for copper oxide thin films before and after annealing are presented in Figure 3(a–c). The as-deposited film shows non-uniform (irregular shapes) without characterized grain boundaries. However, after annealing at 400°C, the morphology changes to the rod-like structures. These nanorods' average width and length were about 92 nm and 438 nm, respectively. At an annealing temperature of 500°C, the CuO nanorods tend to combine to form bigger nano-structures with an approximate width and length of 121 and 360 nm, as demonstrated in Figure 3(c). As presented in Table (1), the role of annealing is to increase the size of CuO crystals in the films. These findings are consistent with a previous article [26].

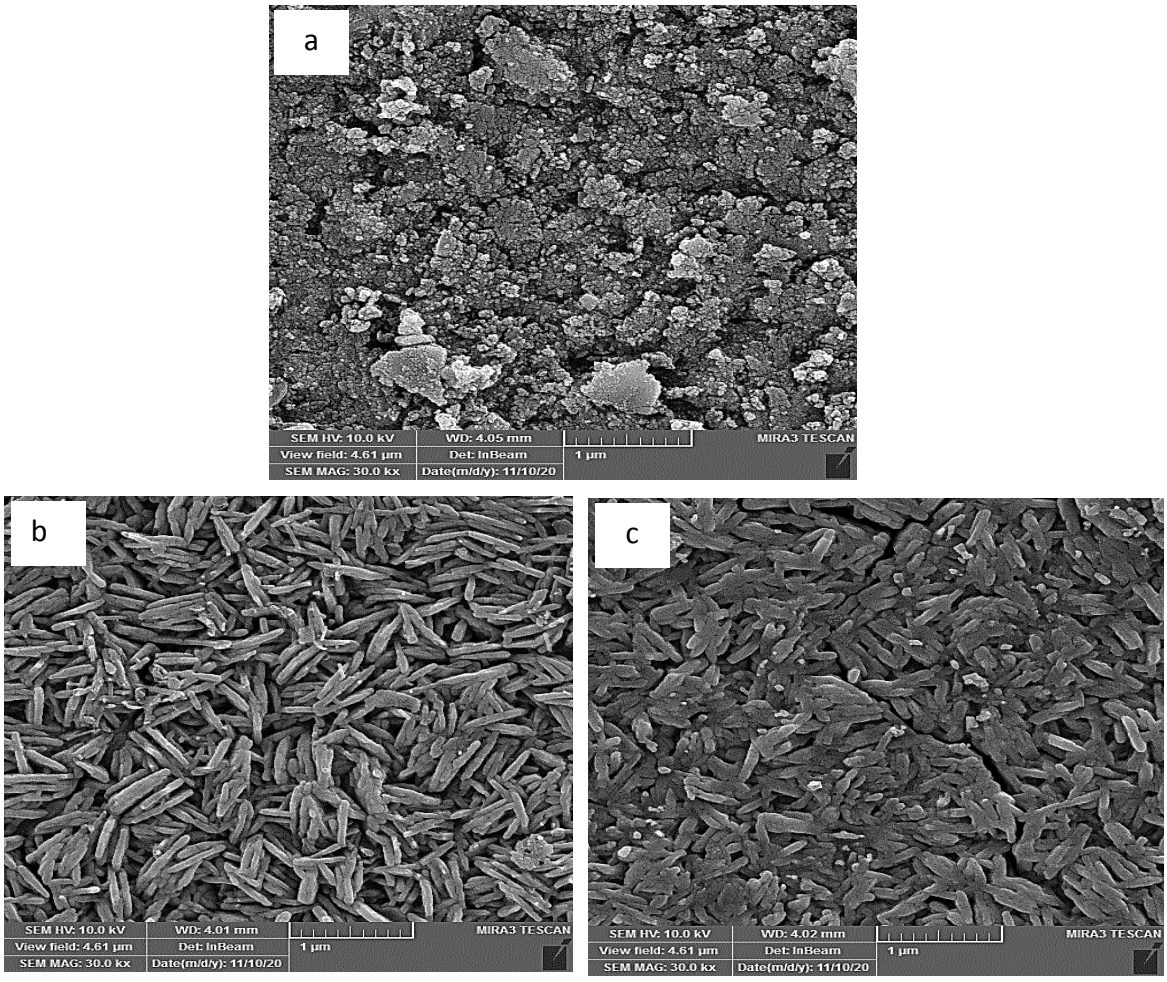

Figure 4: FESEM photos of CuO thin films for (a) as-prepared and after annealing at (b) 400 °C (c) 500 °C

The stoichiometric composition has been studied using energy dispersive spectroscopy (EDS). Figure 4 reveals the existence of both copper and oxygen atoms in the prepared samples. The elemental ratio of Cu for as-deposited and annealed samples at temperatures 400 and 500 ^{o}C are respectively 72.39 %, 78.76 %, and 76.94 %. and for oxygen 25.39 %, 21.24 % and 23.06 % respectively. These results are compatible with a previously reported stoichiometric compound (79.88 % Cu and 20.12 % O) for copper oxide [27]. The AFM technique was used to determine the roughness of the CuO thin films to specify their surface morphology. The AFM images (2D-3D) for CuO before and after annealing are shown in Figure 5. Fine grains were visible in the as-deposited sample, with a root mean squared (RMS) roughness of 2.43 nm. After annealing, both the average grain size and roughness increase. The enhanced values with heat treatment temperature are presented in Table 1. The high values of grain sizes seen in Figures 3 and 5 after annealing may be due to the formation of larger crystallite sizes, as confirmed by XRD analysis [28, 29]. Moreover, due to the formation of rod-like shapes, the differences in the dimensions of these rods increase the roughness.

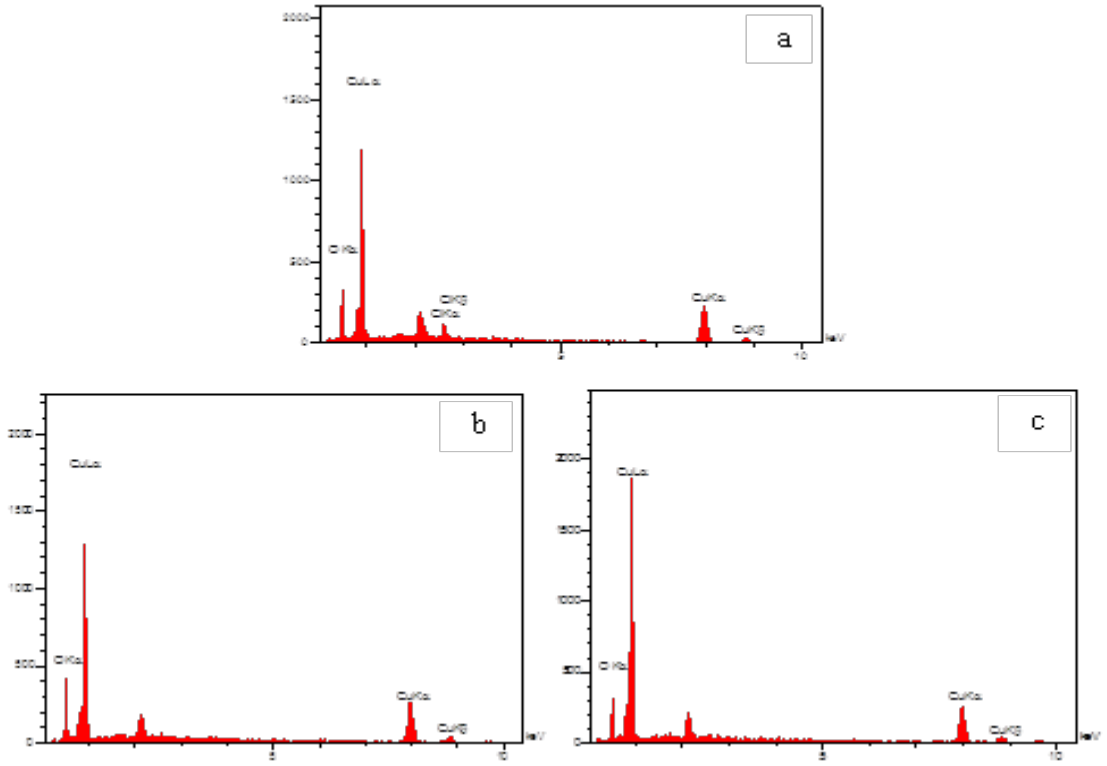

Figure 5: EDS spectra of CuO thin films for (a) as-prepared and after annealing at (b) 400 °C (c) 500 °C

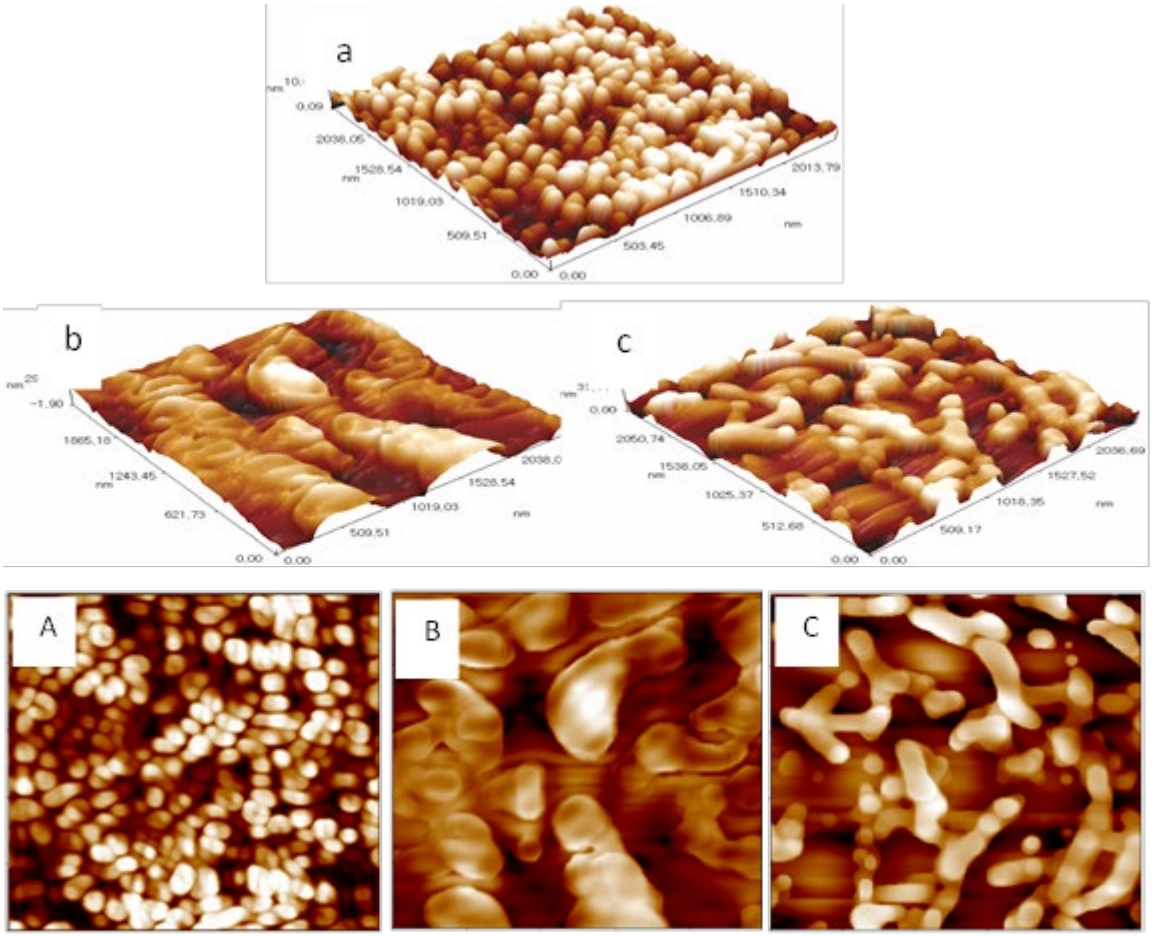

Figure 6: Two (a, b, c) and three dimensional (A, B, C) images of AFM for CuO thin films prepared by CBD. (a) as deposited, (b) at 400°C, and (c) at 500°C

4.3 Optical properties

UV-visible spectra were used to investigate the optical properties and determine the optical bandgap energy. Figure 6 presents the absorption coefficient data against wavelength for the CuO films prepared by CBD and annealed at two different temperatures. Equation (3) below was used to calculate the absorption coefficient values [30]:

$$\alpha = \frac{1}{d} 1n \frac{1}{T} \tag{7}$$

where *d* and *T* are respectively the thickness and the transmittance of the thin film.

Figure 6 depicts the absorption coefficient versus wavelength for CuO thin films prepared by the CBD technique and annealed at two temperatures. The absorption coefficient is higher in the short wavelength part of the visible spectrum. It also shows that as the deposition temperature rises, the absorbance of CuO thin films rises. This may be due to the conversion of the stoichiometry from Cu_2O to CuO, where the Cu_2O has a lower absorption coefficient. This is in agreement with a previous study [31]. The Urbach energy is related to defects' density, which is responsible for the additional levels inside the optical bandgap. The Urbach energy of films is affected by increasing the temperature of the annealing process. Figure 7 shows the decrease in the energy of the tails when the temperature is increased. The measured values are (0.526 eV, 0.460 eV, and 0.355 eV). and the reason is that the heat treatment increases the crystallite size. Hence, the energy of the tails decreases [32]. Tauc's equation was utilized to calculate the optical bandgap of the films [33]

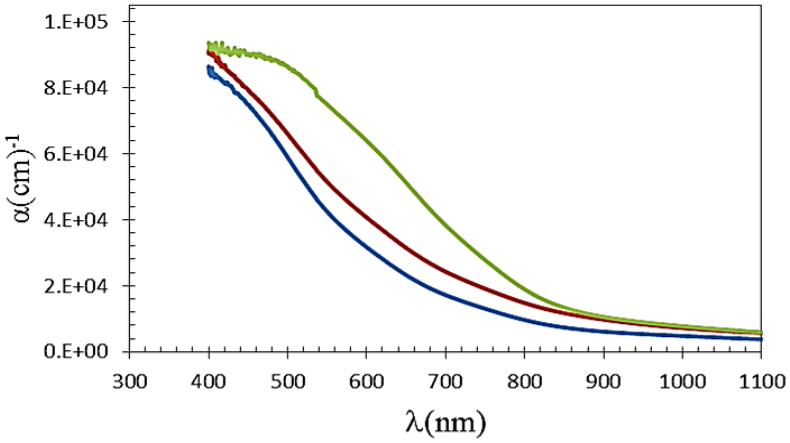

Figure 7: Absorption coefficient values of CuO prepared by CBD of the as-deposited, 400°C, and 500°C annealed samples

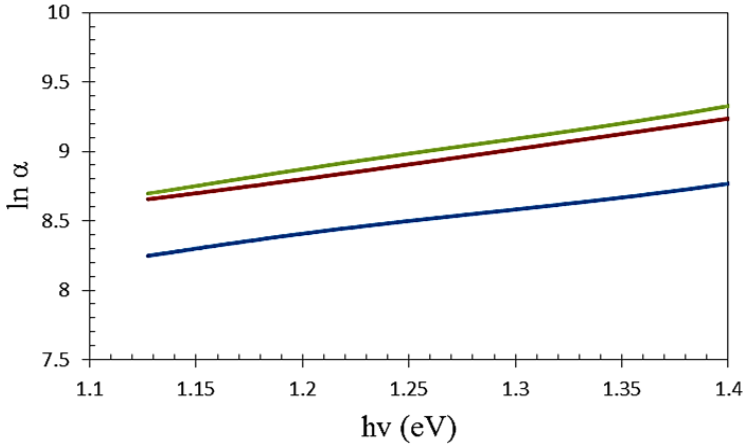

Figure 8: Urbach-energy of CuO thin films for as-deposited and annealed samples at 400°C and 500°C.

$$ahv = \eta \left(hv - E_g\right)^{1/2} \tag{8}$$

where η is a constant, α is the absorption coefficient, $h\nu$ is the incident photon's energy, E_g is the optical bandgap $r = \frac{1}{2}$ for the allowed direct transitions. Figure 8 reveals how to use Eq.(8) to calculate the value of the bandgap energy. The intercept points in the figure are 2.1, 1.61, and 1.63 eV for the as-deposited and the annealed samples at 400°C and 500 °C, respectively. Annealing at 400°C and 500 °C reduces the optical bandgap, which may be attributed to the increased crystallinity resulting from the reduced number of structural defects and enhancement of CuO phase at the expense of Cu_2O phase. The calculated CuO

bandgap values are similar to those found in reference [34]. Reducing the bandgap energy of CuO is important in photovoltaic applications. For example, as an absorption layer in solar cells, a thin film with a small bandgap is a good candidate.

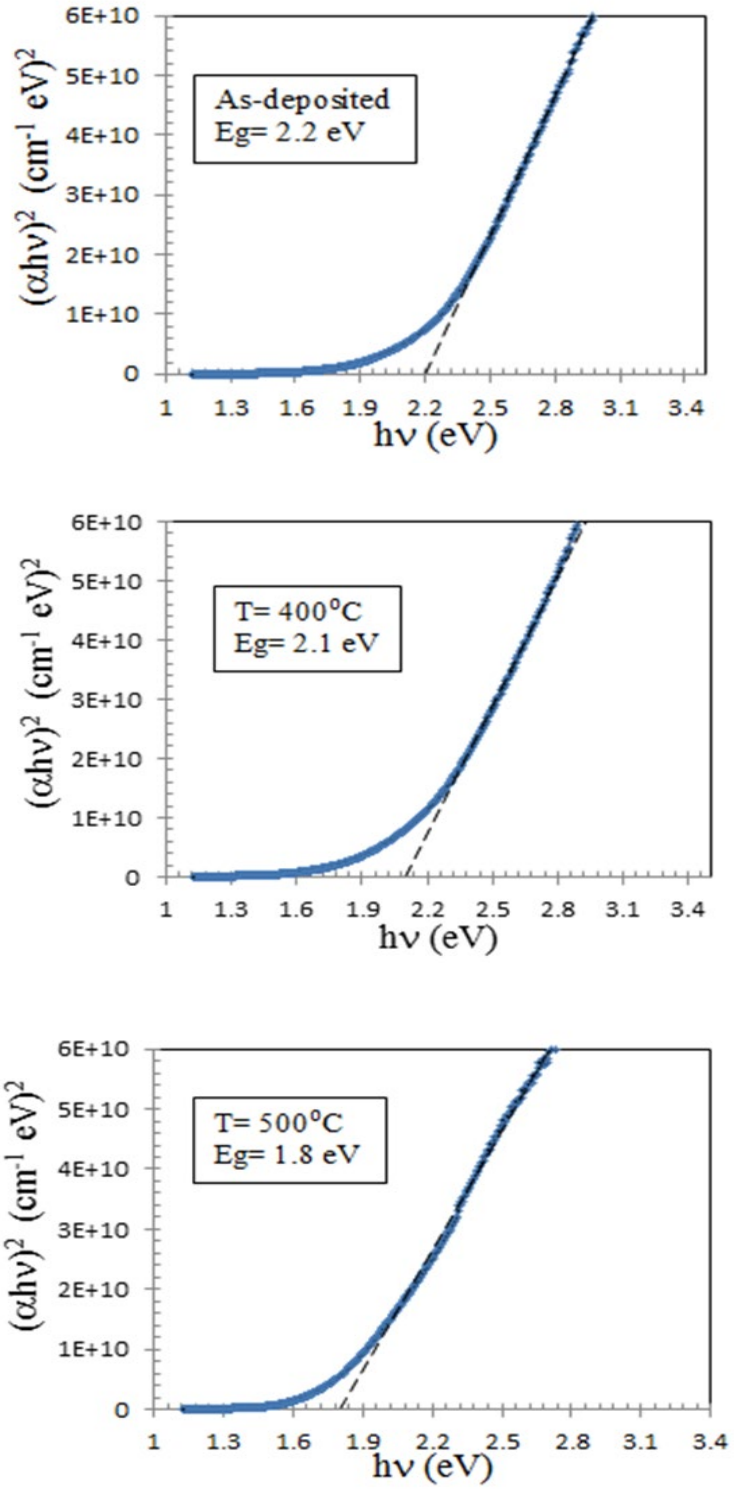

Figure 9: Tauc-plots for CuO films before and after annealing at T=400 and 500 °C for 2 hours

5. Conclusions

A simple, relatively low temperature and economical chemical bath deposition method can be used to prepare CuO thin films. The structure, morphology, and optical properties of the CuO thin films have been investigated with regard to annealing temperature. The XRD results revealed an increase in crystallite size with annealing temperature. SEM analysis shows the conversion of the irregular nano-shapes to nanorods with more regular shapes by annealing. The AFM images show that the nano-structure size of RMS increases with heat treatment. The absorption coefficient increases with annealing due to turning the

Cu_2O to CuO, where the Cu_2O has a lower absorption coefficient. After annealing, the bandgap values are reduced from 2.1 to about 1.62 eV, as confirmed by the optical analysis.

Author contribution

All authors contributed equally to this work.

Funding

This research received no specific grant from any funding agency in the public, commercial, or not-for-profit sectors.

Data availability statement

The data that support the findings of this study are available on request from the corresponding author.

Conflicts of interest

The authors declare that there is no conflict of interest.

References

[1] Y. Y. Wu, W. C. Tsui, T. C. Liu, Experimental analysis of tribological properties of lubricating oils with nanoparticle additives, Wear, 262 (2007) 819–825. https://doi.org/10.1016/j.wear.2006.08.021

[2] C. M. Muiva, K. Maabong, C. Moditswe, CuO nanostructured thin films synthesised by chemical bath deposition on seed layers deposited by successive ionic layer adsorption and reaction and chemical spray pyrolysis techniques, Thin Solid Films, 616 (2016) 48–54. https://doi.org/10.1016/j.tsf.2016.07.061

[3] Q. Zhang,, K. Zhang, D. Xu, G. Yang, H. Huang, F. Nie, C. Liu, S. Yang, CuO nano-structures: synthesis, characterization, growth mechanisms, fundamental properties, and applications, Prog. Mater. Sci., 60 (2014) 208-337. https://doi.org/10.1016/j.pmatsci.2013.09.003

[4] H. B. Oh, H. Ryu, W. J. Lee, Effects of growth temperature on cupric oxide nanorod photoelectrodes using a modified chemical bath deposition, J. Electrochem. Soc., 161 (2014) H633–H636.

[5] Z. Li, , J. Wang, , N. Wang, S. Yan, W. Liu, Y. Fu, Z. Wang, Hydrothermal synthesis of hierarchically flower-like CuO nanostructures with porous nanosheets for excellent H2S sensing, J. Alloys Compd., 725 (2017) 1136-1143. https://doi.org/10.1016/j.jallcom.2017.07.218

[6] A. Zúñiga, L. Fonseca, J. A. Souza, C. R. Gomez, C. D. Pomar, D. Criado, Anomalous ferromagnetic behavior and size effects in CuO nanowires, J. Magn. Magn. Mater., 471 (2019) 77–81. https://doi.org/10.1016/j.jmmm.2018.09.048

[7] L. Arfaoui, F. Janene, S. Kouass, S. Mignard, F. Touati, H. Dhaouadi, CuO nanosheets: synthesis, characterization, and catalytic performance, Russ. J. Inorg. Chem., 64 (2019) 1687–1696. https://doi.org/10.1134/S0036023619130060

[8] K. R. Park, H. B. Cho, J. Lee, Y. Song, W. B. Kim, Y. H. Choa, Design of highly porous SnO_2-CuO nanotubes for enhancing H_2S gas sensor performance, Sensors. Actuators, B Chem., 302 (2020) 127179. https://doi.org/10.1016/j.snb.2019.127179

[9] M. Makenali , I. Kazeminezhad, Characterization of thin film of CuO nanorods grown with a chemical deposition method: a study of significance of deposition time, Inorg. Nano-Metal Chem., 50 (2020) 764–769. https://doi.org/10.1080/24701556.2020.1724149

[10] S. Anantharaj, H. Sugime, S. Noda, Ultrafast growth of a $Cu(OH)_2$-CuO nanoneedle array on Cu foil for methanol oxidation electrocatalysis, ACS Appl. Mater. Interfaces, 12 (2020) 27327–27338. https://doi.org/10.1021/acsami.0c08979

[11] M. Yang , J. He, Fine tuning of the morphology of copper oxide nano-structures and their application in ambient degradation of methylene blue, J. Colloid Interface Sci., 355 (2011) 15–22. https://doi.org/10.1016/j.jcis.2010.11.022

[12] Q. Liu, H. Liu, Y. Liang, Z. Xu, G. Yin, Large-scale synthesis of single-crystalline CuO nanoplatelets by a hydrothermal process, Mater. Res. Bull., 41 (2006) 697–702. https://doi.org/10.1016/j.materresbull.2005.10.013

[13] V. R. Katti, A. K. Debnath, K. P. Muthe, M. Kaur, A. K. Dua, S. C. Gadkari, S. K. Gupta , V. C. Sahni, Mechanism of drifts in H_2S sensing properties of SnO_2: CuO composite thin film sensors prepared by thermal evaporation, Sens. Actuators B Chem., 96 (2003) 245-252. https://doi.org/10.1016/S0925-4005(03)00532-X

[14] J. T. Chen, F. Zhang, J. Wang., G. A. Zhang, B. B. Miao, X. Y. Fan, D. Yan , P. X. Yan, CuO nanowires synthesized by thermal oxidation route, J. Alloy. Compd., 454 (2008) 268-273. https://doi.org/10.1016/j.jallcom.2006.12.032

[15] J. Zhu, D. Li, H. Chen, X. Yang, L. Lu, X. Wang, Highly dispersed CuO nanoparticles prepared by a novel quick-precipitation method, Mater. Lett., 58 (2004) 3324–3327. https://doi.org/10.1016/j.matlet.2004.06.031

[16] Z. Yang, J. Xu, W. Zhang, A. Liu, S. Tang, Controlled synthesis of CuO nano-structures by a simple solution route, J. Solid State Chem., 180 (2007) 1390–1396. https://doi.org/10.1016/j.jssc.2007.02.008

[17] M. A. Dar, Q. Ahsanulhaq, Y. S. Kim, J. M. Sohn, W. B. Kim, H. S. Shin, Versatile synthesis of rectangular shaped nanobat-like CuO nano-structures by hydrothermal method; structural properties and growth mechanism, Appl. Surf. Sci., 255 (2009) 6279–6284. https://doi.org/10.1016/j.apsusc.2009.02.002

[18] B. Singh , S. K. Tiwary, CuO Thin Film Prepared by Chemical Bath Deposition Technique : A Review, J. Nanosci. Nanotechnol., 8 (2017) 11–15.

[19] J. w. Ha, J. Oh, H. Choi, H. Ryu, W. J. Lee, J. S. Bae, Photoelectrochemical properties of Ni-doped CuO nanorods grown using the modified chemical bath deposition method, J. Ind. Eng. Chem., 58 (2018) 38–44. https://doi.org/10.1016/j.jiec.2017.09.004

[20] H. B. Oh, H. Ryu, W. J. Lee, Effects of copper precursor concentration on the growth of cupric oxide nanorods for photoelectrode using a modified chemical bath deposition method, J. Alloys Compd., 620 (2015) 55–59. https://doi.org/10.1016/j.jallcom.2014.09.108

[21] L. Liu, K. Hong, T. Hu, M. Xu, Synthesis of aligned copper oxide nanorod arrays by a seed mediated hydrothermal method, J. Alloys Compd., 511 (2012) 195–197. https://doi.org/10.1016/j.jallcom.2011.09.028

[22] A. S. Dive, K. P. Gattu, N. P. Huse, D. R. Upadhayay, D. M. Phase, R. B. Sharma, Single step chemical growth of ZnMgS nanorod thin film and its DFT study, Mater. Sci. B Eng., 228 (2018) 91–95. https://doi.org/10.1016/j. Nanosci. Nanotechnol mseb.2017.11.018

[23] G.Hodes, Chemical Solution Deposition of Semiconductor Films, Marcel Dekker, Inc., 1st ed, New York, 2002.

[24] B. Sahin , T. Kaya, Enhanced hydration detection properties of nanostructured CuO films by annealing, Microelectron. Eng., 164 (2016) 88–92. https://doi.org/10.1016/j.mee.2016.07.016

[25] D. Gopalakrishna, K. Vijayalakshmi, C. Ravidhas, Effect of annealing on the properties of nanostructured CuO thin films for enhanced ethanol sensitivity, Ceram. Int., 39 (2013) 7685–7691. https://doi.org/10.1016/j.ceramint.2013.03.021

[26] K. Sahu, S. Choudhary, S. A. Khan, A. Pandey, S. Mohapatra, Thermal evolution of morphological, structural, optical and photocatalytic properties of CuO thin films, Nano-Structures , Nano-Objects, 17 (2019) 92–102. https://doi.org/10.1016/j.nanoso.2018.12.005

[27] I.K.Uthman, I.K.Ahmadu, U.Uno, E. Uno, Effect of oxidation temperature on the properties of copper oxide thin films prepared from thermally oxidised evaporated copper thin films, J. Appl. Phys., 3 (2013) 61-66.

[28] J. Y. Park, T. H. Kwon, S. W. Koh, Y. C. Kang, Annealing temperature dependence on the physicochemical properties of copper oxide thin films, Bull. Korean Chem. Soc., 32 (2011) 1331–1335. https://doi.org/10.5012/bkcs.2011.32.4.1331

[29] S. Venkataraj, O. Kappertz, C. Liesch, R. Detemple, R. Jayavel, M. Wuttig, Thermal stability of sputtered zirconium oxide films, Vacuum, 75 (2004) 7–16. https://doi.org/10.1016/j.vacuum.2003.12.127

[30] M. Amalina , M. Rusop, Morphological, electrical and optical properties of γ- copper (I) iodide thin films by mist atomization technique, World J. Eng., 9 (2012) 251–256. https://doi.org/10.1260/1708-5284.9.3.251

[31] R. D. Prabu, S. Valanarasu, V. Ganesh, M. Shkir, S. AlFaify, A. Kathalingam, S. R. Srikumar, R. Chandramohan, An effect of temperature on structural, optical, photoluminescence and electrical properties of copper oxide thin films deposited by nebulizer spray pyrolysis technique, Mat. Sci. Semicon. Proc., 74 (2018) 129-135. https://doi.org/10.1016/j.mssp.2017.10.023

[32] A. N. Hussain, K. I. Hassoon, M. A. Hassan, Effect of Annealing on Copper Oxide Thin Films and Its Application in Solar Cells, J. Phys. Conf. Ser.,1530 (2020) 012140. http://dx.doi.org/10.1088/1742-6596/1530/1/012140

[33] F. Bayansal, B. Şahin, M. Yüksel, N. Biyikli, H. A. Çetinkara, H. S. Güder, Influence of coumarin as an additive on CuO nano-structures prepared by successive ionic layer adsorption and reaction (SILAR) method, J. Alloys Compd., 566 (2013) 78–82. https://doi.org/10.1016/j.jallcom.2013.03.018

[34] A. Bouich, S. Ullah, H. Ullah, B. Mari, M. E. Touhami, B. Hartiti, D. S. Santos, Optoelectronic characterization of CuIn(S,Se)2 thin grown by spray pyrolysis method for solar cells, Int. Ren. Sus. E. Conf., 2018, 1-5. https://doi.org/10.1109/IRSEC.2018.8702992